5th Australasian Congress on Applied Mechanics, ACAM 2007
10-12 December 2007, Brisbane, Australia

Failure of Sandwich Composite Structure Containing Face-sheet/Core Disbonds – An Experimental Study

T. Southward[1], D.P.W. Horrigan[2], G.D. Mallinson[3], K. Jayaraman[3]

[1]*ANZES Design Engineering, Air New Zealand, New Zealand*
[2]*Technical Operations, Air New Zealand, New Zealand*
[3]*Department of Mechanical Engineering, University of Auckland, New Zealand*

Abstract: Honeycomb sandwich specimens containing manufactured circular disbonds were loaded to failure in bending. Particular emphasis was placed on accurately identifying the occurrence of disbond buckling and growth initiation, as these two events are difficult to monitor. The test results are presented and then the methods used to identify disbond buckling and growth initiation are described. The method of identifying disbond buckling was very successful. The method of identifying growth initiation was largely successful but improvements are suggested. Finally, conclusions are presented and recommendations made regarding design and repair considerations. The study was performed to provide data against which predictive models can be validated, filling a large gap in the published literature regarding experimental results for disbonded sandwich structure.

Keywords: buckling, damage tolerance, disbond, failure, growth, sandwich structure, testing.

1 Introduction

Sandwich construction is used extensively in aerospace applications where its high stiffness-to-weight ratio is particularly valuable. The usage of sandwich structures in exterior applications on commercial aircraft (such as control surfaces, fairings and cowlings) is somewhat declining, due in large part to the issues of impact-induced core damage and water ingression into honeycomb cells. Both of these events can cause disbonds that may not be easily detectable by visual inspection. Disbonds are capable of initiating catastrophic structural failure, such as the Airbus A300/310 rudder losses, which were caused by disbonds that propagated during flight. To eliminate these damage mechanisms, some sandwich construction is being replaced by solid composite laminates in 'next generation' aircraft. This is not relevant for interior aircraft applications and sandwich structures continue to be used extensively in interior applications. Certification of both interior and exterior aircraft structures may require consideration of damage tolerance, in which case disbond propagation and resulting panel failure must be understood. This paper presents the results of an investigation into the failure process of sandwich panels containing circular disbonds, loaded in bending. The test specimens are slight variations on a typical aircraft sandwich configuration, having two-ply glass/epoxy face sheets on a 26mm thick, 48kg/m^3 Nomex honeycomb core.

There are no published papers describing generic testing of a honeycomb sandwich panel containing an embedded disbond. The few papers that do describe testing of disbonded sandwich panels are either for specific geometric arrangements or describe only one or two tests [1-3]. The testing in this study was conducted to understand the failure process for typical aircraft sandwich panels and also to establish test methods that may be used in future studies on alternative configurations.

2 Test Specimens

A test matrix was developed using three parameters, each having 2-3 variations (Table 1): (1) Disbond diameter, (2) Face-sheet stiffness, (3) Disbond ratio (ratio of panel width to disbond diameter)

A full factorial test plan would require 12 configurations. A half-factorial plan was used to minimise test requirements; further the effect of disbond ratio was anticipated to be minimal. Four repeats were manufactured for each of the 6 configurations, resulting in a total of 24 test specimens. All specimens were manufactured in accordance with aerospace industry recommended practices (SAE ARP5144 and ARP5143). Circular disbonds were manufactured into each specimen by inserting a layer of PTFE release film between the face-sheet and core. The face-sheet in-plane elastic moduli are 23.4GPa and 22.7GPa for the 'A' and 'B' face-sheets respectively. The face-sheet thicknesses are 0.478mm and

0.420mm for the 'A' and 'B' face-sheets, respectively. Complete material data and specimen geometries can be found in [4].

Table 1 – Half-factorial test plan for panel specimens

Configuration	Disbond Diameter	Face-sheet	Disbond Ratio
25-A-4	25 mm	A	4
25-B-2	25 mm	B	2
50-A-2	50 mm	A	2
50-B-4	50 mm	B	4
75-A-4	75 mm	A	4
75-B-2	75 mm	B	2

3 Specimen Loading and Failure Process

All test panels were loaded in four-point bending, Figure 1, such that the disbonded region was in compression. Loading was continued until failure, which was defined as gross loss of structural stiffness.

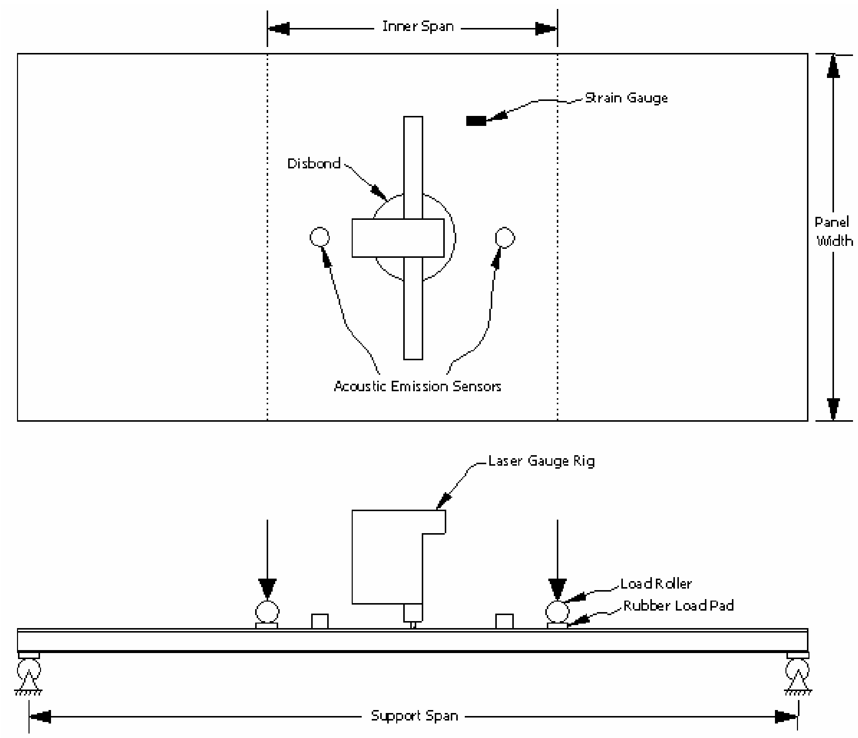

Figure 1 – Test specimen arrangement

The main reason for selecting a bend test configuration over a pure compression configuration is that sandwich panels are typically used in applications in which they are loaded in bending. Furthermore, one of the features of pure-compression load tests is that global buckling and disbond buckling are inextricably linked. When considering a thick sandwich panel (relative to its length), for which the panel buckling load is significantly larger than the wrinkling load, it is reasonable to decouple the face-sheets and consider the localised behaviour of the disbond without considering the global panel behaviour. The range of panel dimensions for which this decoupling is reasonable is not the subject of this research and could not be determined from a review of the literature. It is stated only for consideration and to illustrate that bend testing, in which panel buckling does not occur, can not only model the behaviour of panels in bending but also the behaviour of a range of pure-compression panels. The reverse is not true of pure-compression testing. This is the justification for the use of a four-point bending configuration.

For all tested specimens, the failure process consisted of the following steps: (1) Buckling of the disbonded face-sheet; (2) Approximately 2-5 small increments of disbond growth perpendicular to the loading direction; (3) Unsteady disbond growth through the entire specimen width, causing gross loss of stiffness

The load at which each of these events occurred for each test configuration is presented in Table 2. All loads were derived from strain gauge output. Each result is the average of four repeats of each test configuration and is presented with a confidence range. This is the range within which the population mean is expected to lie with 95% confidence [4]. The growth initiation loads display significantly higher scatter than the buckling and failure loads due largely to the variability in fracture behaviour. The remaining sections of this paper will describe the methods of determining the buckling loads and the growth initiation loads.

Table 2 – Test Result Summary

Specimen Designation	**Buckling Load (N/m)**		**Growth Initiation Load (N/m)**		**Failure Load (N/m)**	
	Mean	Conf. Range	Mean	Conf. Range	Mean	Conf. Range
25-A-4	24900	± 3.6%	42722	± 19.8%	54333	± 6.4%
25-B-2	17144	± 8.1%	26756	± 25.4%	38438	± 7.6%
50-A-2	7832	± 7.4%	28000	± 25.4%	40092	± 5.0%
50-B-4	4849	± 13.6%	14242	± 62.8%	27992	± 10.6%
75-A-4	3385	± 20.9%	21313	± 13.2%	33975	± 10.0%
75-B-2	1894	± 19.7%	14727	± 18.7%	25245	± 6.2%

The loads in Table 2 for all specimens with 'A'-type face-sheets are plotted in Figure 2 normalised to the wrinkling load of the panel, i.e. undamaged failure load.

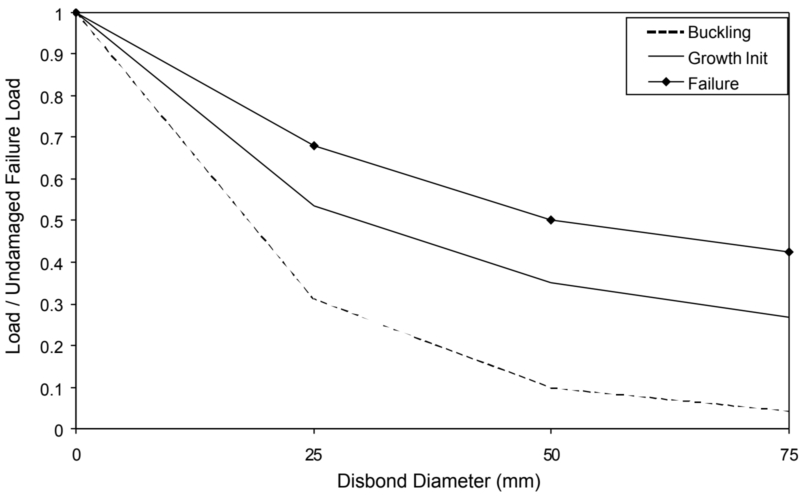

Figure 2 – Normalised buckling, growth initiation and failure loads for thick face-sheet panels

The following general observations were made regarding the failure process:

- Failure occurred when disbond growth became unstable and the disbond propagated through the entire panel width (extending in the loading direction also). The face-sheet remained intact in all cases and failure was defined as gross loss of stiffness.
- The disbond front propagated predominantly through the core material, just below the resin fillets.
- The reduction in panel stiffness throughout testing was less than 5% in all cases.
- The bending stiffness of the B face-sheet is 67% that of the A face-sheet. The average ratios of B-to-A loads for buckling, growth initiation and failure were 62%, 61% and 72%, respectively.

Therefore, buckling, growth initiation and failure loads are all approximately proportional to face-sheet bending stiffness.

4 Method for Identifying Disbond Buckling

For sandwich panels with embedded disbonds the difference between the pre and post-buckling structural stiffness was found to be negligible (particularly for a small disbond in a wide panel). It is therefore not possible to determine accurately the occurrence of buckling from the load profile. Disbond buckling is defined as the point at which the disbonded face-sheet deflects out-of-plane. To capture this event for the panel specimens, a laser displacement gauge was mounted in a rig, which enabled the measurement of the out-of-plane displacement of the centre of the disbond. As well as determining the onset of buckling, this also provided a complete record of the maximum disbond height throughout the loading process (Figure 3).

A mounting rig was built to hold a laser gauge directly above the centre of a circular disbond and to allow it to translate in the out-of-plane direction as the panel was loaded (Figure 1). The rig was supported by two pins located on a line perpendicular to the length of the beam, enabling the measurement of the relative ‘height’ of the buckled disbond. To allow the rig to move up and down smoothly and stay permanently in contact with the specimen, a linear bearing assembly was used. The bearing assembly was realigned prior to each test to ensure that the laser gauge was free to slide vertically, maintaining contact with the specimen at all times. The additional panel loading due to the laser gauge mass was negligible (approximately 10N).

A typical plot of buckle height (laser gauge output) versus face-sheet load illustrates the method of determining buckling load from the laser gauge output.

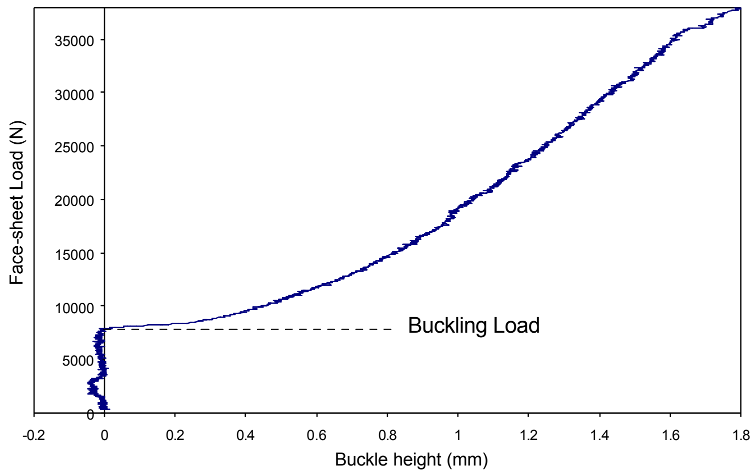

Figure 3 – Identification of buckling load from laser gauge output

The relationship between face-sheet load and disbond height in post-buckling was found to be approximately parabolic. Of the 24 specimens tested, 7 exhibited snap buckling, which is the result of the disbond buckling towards the core initially and then, at a load higher than the buckling load, ‘snapping’ outwards to form a typical buckle. To determine the buckling load for such specimens from laser gauge results, the parabolic relationship between face-sheet load and buckle height was used to interpolate the profile to a buckle height of zero.

5 Method for Identifying Disbond Growth Initiation

Disbond growth is particularly difficult to monitor with an embedded disbond because there is little change in panel stiffness and no visual access to the growth front. Some form of non-destructive inspection is required to capture disbond growth events. Preliminary testing indicated that the only clear evidence of disbond growth was a visible increase in the plan area of the buckled face-sheet accompanied by audible noise associated with fracture. It was decided that the noise associated with fracture would be a more reliable means of identifying disbond growth events and consequently acoustic emission monitoring was employed.

5.1 Acoustic Emission Data

The arrangement of acoustic emission sensors is shown in Figure 1. A Vallens AMS-3 4 channel acquisition unit with SE45-H transducers, having a range of 25kHz to 260kHz, was used to monitor acoustic emissions. The range of the transducers is outside the audible range but they can accurately identify fibre fracture events, which typically occur in this frequency range [Pappas et al.]. The raw acoustic emission data for each test consisted of up to 3000 acoustic events sampled at 5 MHz, approximately 25% of which were stored as transient files containing the full waveform of the acoustic event. For the remaining 75% of acoustic events, some general features such as rise time, duration, counts, amplitude and energy were recorded. How these acoustic features were used to identify disbond growth is the subject of the following sections.

5.2 Cumulative Acoustic Event Count

Prior to testing it was assumed that the amount of acoustic activity would increase significantly when the disbond began to grow. The test results proved this to be generally true, with a ten-fold increase in cumulative acoustic counts in the last 10% of the test duration. However, there was also typically a visible and audible stable disbond growth event before the rapid increase in cumulative acoustic counts. To accurately identify the first disbond growth event, an analysis of the individual acoustic events was performed.

5.3 Time Domain Analysis

The analysis of acoustic events in order to identify particular damage types is a developing field of study. In the specific area of fibre fracture in composite materials, several methods of correlating acoustic signals with fibre fracture have been identified [5]. The first of these methods is in the time domain, and defines two parameters based on an acoustic event profile; (1) the average frequency (*AvF*), defined as the number of counts in an acoustic event divided by the event duration, (2) the threshold amplitude fraction (*THA*), defined as the threshold amplitude of the acoustic event divided by the maximum amplitude in the duration of the event.

Using these parameters and investigation of test data, a criterion for identifying a disbond growth event was defined. Acoustic events in which *AvF* was between 40kHz and 70kHz and *THA* was less than 0.7 were defined as events resulting from disbond growth. The criterion was developed based on the following observations:

- Of the events satisfying the growth criterion none occurred before buckling. Given that there is no disbond growth before buckling, this is a necessary observation to validate the criterion.
- It was observed during loading of the test specimens that there were one or two audible events accompanied by visible disbond growth. The audibility of these events indicated that they would show up as the highest-energy events in the AE data. Of the highest-energy acoustic events in each test, 79% satisfied the growth criterion, while only 6% of all acoustic events satisfied the growth criterion.
- In all of the tests a step increase in the cumulative number of acoustic counts corresponded with the occurrence of an event satisfying the growth criterion.
- Utilisation of the criterion resulted in consistent growth initiation load predictions.

It is likely that some events satisfying the growth criterion were not disbond growth events and that some growth events were not captured by the criterion. The statistical rigor of the criterion cannot be assessed due to the relatively small amount of data collected and the lack of benchmark growth events. To obtain a more definitive criterion for disbond growth, it is recommended that core, face-sheet and interfacial bond fracture should be monitored in isolation. Further investigation of events satisfying the growth criterion was performed using a frequency analysis of the transient signals, as described in the next section.

5.4 Frequency Content of the Acoustic Events

For each test, approximately 25% of the acoustic events were recorded at 5MHz and stored as 'transient' files, in which the complete waveform was recorded. The Fast Fourier Transform algorithm was used to extract the frequencies from each transient waveform. By far the most dominant frequencies (in terms of signal amplitude) in all transient files were 195 kHz, 186 kHz and, to a lesser extent 168 kHz. The propagation frequencies for S-Glass are 136 kHz, 176 kHz and 360 kHz [5]. The fibres in the face-sheet are E-glass, which has a modulus and density similar to that of S-Glass. It is considered likely that the dominant frequencies observed in testing are propagation frequencies of the face-sheet material rather than a signature of the disbond growth event.

Analysis of the frequency peaks for all transients compared with only those transients satisfying the growth criterion failed to conclusively identify any frequencies specific to disbond growth events. A number of methods were used in an attempt to isolate frequencies specific to disbond growth, but the number of transient files analysed was too small and the variation too large to isolate trends with a reasonable level of statistical significance.

6 Conclusions and Recommendations

- Failure due to disbonding is initiated by disbond buckling, which establishes a mode I mechanism for disbond growth. Small increments of disbond growth initiate at loads significantly higher than the buckling load. Failure, defined as a gross loss of stiffness, is caused by unstable disbond growth through the entire panel width.
- The difference between pre and post-buckling panel stiffness was negligible in all cases
- The reduction in load carrying capacity due to the presence of disbonds was between 32% and 64% for the tested specimens.
- Disbond buckling was accurately captured using a specially mounted laser displacement gauge
- An acoustic criterion for disbond growth was developed and resulted in consistent growth initiation loads. The criterion has not been validated as part of this study and it is recommended that, if acoustic emission is to be used for growth monitoring, isolated testing should be done to characterise the acoustic signal of disbond growth with a higher degree of certainty.
- The failure load was found to be linearly proportional to face-sheet bending stiffness. Therefore, a simple bonded patch one half the thickness of the face-sheet, applied over the disbond region would increase the damaged panel load carrying capacity by 238%, easily restoring the original panel strength for the range of disbond sizes tested.
- In damage tolerance terms, the buckling load represents the endurance limit. The growth initiation load represents limit load capability for aircraft design.
- This study has developed results suitable for validation of numerical models. The key events that should be predicted by a complete analysis are buckling, growth initiation and failure due to unstable disbond growth. Details of such predictive analysis are contained in [4].

7 Acknowledgements

This project was completed with funding from the Foundation for Research Science and Technology, New Zealand. Acoustic emission equipment and expertise were supplied by Industrial Research Limited, Auckland.

8 References

[1] Han, T.S., Ural, A., Chen, C.S., Zehnder, A.T., Ingraffea, A.R., Billington, S.L., 2002. Delamination buckling and propagation analysis of honeycomb panels using a cohesive element approach. *International Journal of Fracture*, 115: 101-123.

[2] Hansen, U. 1998. Compression behaviour of frp sandwich specimens with interface debonds. *Journal of Composite Materials*, 32(4): 335-360.

[3] Falk, L. 1994. Foam core sandwich panels with interface debonds. *Composite Structures*, 28(4): 481-490.

[4] Southward, T. 2005. Buckling and growth of disbonds in honeycomb sandwich structure. PhD thesis. The University of Auckland, New Zealand.

[5] Pappas, Y.Z., Kontsos, A., Loutas, T.H., Kostopoulos, V. 2004. On the characterisation of continuous fibres fracture by quantifying acoustic emission and acousto-ultrasonic waveforms. *NDT&E International*, 37: 389-401